# Fabrication of Parallel Compliant Mechanisms via Additive Manufacturing

Alberto Parmiggiani[1], Divya Shah[1] and Giovanni Berselli[12]

[1] Fondazione Istituto Italiano di Tecnologia (IIT), Via S. Quirico 19/D, 16163 Genova, Italy

[2] University of Genova, Via all'Opera Pia 15/A, 16145 Genova, Italy

June 9, 2023

**Abstract**

The manufacturing and assembly of small parallel mechanisms are often complex because of the required tolerances and high part count. The present work focuses on the use of additively manufactured compliant mechanisms to overcome some of these difficulties. As a reference, this work considers a recent work on a two degrees of freedom parallel orientational mechanism. Several aspects related to the design and manufacturing of this type of small-scale system are addressed by considering two implementations of the mechanism, one developed following a "traditional" approach with linkages and pin joints, and the other developed following a "flexible" approach using additively manufactured flexures. The two versions of the mechanism are finally compared to provide qualitative and quantitative indications of their motion precision and capacity to withstand loads.

***Keywords***— Additive manufacturing, Parallel kinematics, Compliant mechanisms, Flexure hinges

## 1 Introduction

Parallel mechanisms provide several advantageous properties such as greater rigidity, higher speeds, lesser sensitivity to input errors [1], and synergistic behaviour in load distribution when compared to serial ones. These advantages generally come at the cost of mechanical complexity; the manufacturing and assembly of these mechanisms are thus quite challenging. Since parallel mechanisms comprise kinematic loops, their components need to mate with high precision, requiring tight

tolerances, which are generally expensive. Moreover, only traditional CNC processes allow fabrication with these tolerances that are instead difficult to obtain when employing additive manufacturing (AM).

Furthermore, tolerance selection is generally tricky, as the designer needs to strike the right balance between making an easily assemblable mechanism and minimizing the overall amount of backlash. In this typical trade-off situation, the resulting system likely has either too much friction or too much backlash. If at all possible, finding the sweet spot is indeed difficult.

A possible alternate solution to overcome this issue is to replace the joints of parallel mechanisms with compliant joints, thus turning them into compliant mechanisms. This field has been studied widely over the past two decades: the books by Howell [2, 3] and Lobontiu [4] provide comprehensive overviews of as well as coverage of design approaches and guidelines along with several examples of compliant mechanisms and their applications.

The application of compliant mechanisms poses some interesting challenges. Indeed most mechanical systems require relatively large ranges of motion which are difficult to obtain with compliant mechanisms whose strain directly affects their durability and robustness. It is, therefore, interesting to consider the solutions to this problem that are available in the literature.

The approaches can be categorized in many ways, e.g. by the type of manufacturing strategy (subtractive manufacturing, composites formation, and additive manufacturing) or of material employed (metals, plastics, and composites) The following subsections will cover previous works grouping them into four broad categories by the type of manufacturing strategy employed.

## 1.1 Laminae "Cut and Fold"

Some of the earliest implementations of compliant mechanisms in mechatronic devices can be found in the work of Shimada [5] et al. In these works, the authors relied on cutting and folding of thin sheet metal plates.

Since the amount of strain obtained by the repeated bending of metal laminae was limited, the "cut-and-fold" approach was refined in the works of Fearing, Wood et al. with the adoption of laminated composites in a process dubbed "Smart Composite Microstructures" (SCM). The materials used for the flexible part of the joint were mainly Nylon and PET, while the rigid part was made in carbon fibre, fibreglass [6, 7] but also stiff cardboard [8] and posterboard [9]. Researchers demonstrated that this approach is suitable for the fabrication of "micro-robots" and "meso-robots" with remarkable mobility. Recently the same approach has seen implementations in miniature robots for surgery [10] and haptics [11, 12].

The work presented in the patent by Gosselin [13] is also reminiscent of SCM. In this case, Gosselin proposed obtaining the flexible element either with textile tapes or with properly arranged cables.

## 1.2 Subtractive Manufacturing

A different approach adopted, for example by Henein et al. [14], was to form metallic materials from bulk with Electric Discharge Machining (EDM). Naves et al. [15] started from the "butterfly" hinge design by Henein et al. to develop the flexure-based suspension for an iron core direct drive torque motor with a range of motion of 60°.

## 1.3 Additive Manufacturing

Other approaches for constructing compliant joints with large displacements take advantage of the design freedom allowed by AM [16]. Along these lines, several interesting examples can be found in the literature. Fowler et al. presented an evolution of the "butterfly-hinge" design by Henein et al., fabricated via additive manufacturing in titanium [17]. Merriam et al. developed a monolithic 2DOF pointing mechanism [18] for space applications. Kiener et al. presented the construction of a flex type pivot with interlocked flexure blades [19] and a compliant rotation reduction mechanism. Parvari Rad et al. proposed a novel spherical flexure for application on spherical, additviely manufactured compliant mechanisms [20], whereas a design solution aimong at achieveing an isotropic behaviour can be found in [21]. At last, a contact-aided cross-axis pivot, also produced via AM, has been described in [22].

Examples of the use of printed plastic parts are found in the work of Sharkey et al. [23] that presents a monolithic 3D printed flexure translation stage, that forms the key element of an open-source miniature microscope. The component was fabricated via Fused Filament Fabrication (FFF). Almeida et al. [24] also presented a 3D printed flexure-based robotic microtweezers device for precision manipulation that is obtained with Selective Laser Sintering (SLS).

## 1.4 Hybrid manufacturing strategies

An alternate approach to creating flexible hinges is to locally tune the material properties of a structure. In Shape Deposition Manufacturing (SDM) [25] and Hybrid Deposition Manufacturing (HDM) [26] this is achieved through a multiple step molding process that allows constructing flexure hinges by integrating viscoelastic parts within otherwise rigid structures. Robot legs [27] and underactuated robot hands [28] have, for example, been fabricated successfully with this technique.

A similar result, allowing the fabrication of monolithic "multi-material" parts, is possible with the Polyjet material jetting AM machines. In the works of Bruyas et al. [29], the authors presented a compliant multi-material joint for interventional medical applications. Hughes et al. [30] also exploited this technology to create a multi-material robot hand where the joints were obtained with flexible material; the system was fabricated directly with a Stratasys Connex500 3D printer.

## 1.5 Goal of the current work

The goal of the current work is to advance the state of the art of compliant robots fabricated in plastics via AM. Compared to metal AM and metal EDM cutting, plastic AM is generally a more affordable and accessible process. Also, plastics are generally more tolerant to strain, making them an ideal choice for constructing compliant joints. Compared to SCM, plastic AM has the advantage of being less constrained to geometries to be obtained by folding, thus allowing a bit more design freedom for the development of vertical features. Finally, if compared to SDM and HDM, plastic AM has the advantage of being a simpler process, requiring neither moulds nor component curing, where the components can be fabricated in near net shape.

For these reasons, starting from a recent example of a 2DOF parallel orientational mechanism [31, 32] constructed with a traditional approach, this work considers its fabrication instead via plastic AM. This class of mechanisms is particularly well suited for compliant mechanisms because they have the advantageous characteristic of amplifying displacements. Indeed, a given rotational displacement of the moving platform can be achieved by only half of that rotational displacement at the individual actuated joints. This, in turn, reduces the strains the compliant mechanism is required to withstand.

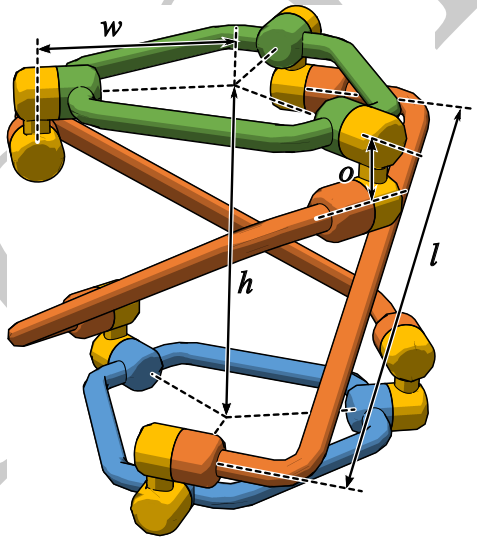


Figure 1: Schematic representation of the proposed 2DPOM and its main geometric parameters.

# 2 Material and Methods

## 2.1 Mechanism Description

The 2DOF parallel orientational mechanism considered for this study, hereafter named *2DPOM*, is inspired by the "quaternion joint mechanism" (as proposed in [31]) and is represented in Fig. 1.

It has a kinematic architecture of three identical "legs" of two universal joints (colored yellow), or equivalently four revolute joints, each diagonally connecting the fixed base (colored blue) to the moving platform (colored green). This arrangement achieves a structure similar to a three-dimensional anti-parallelogram and it emulates the rolling contact motion of two spheres.

The system geometry is fully determined with three independent parameters: $l$, $o$, and $w$. The parameter $l$ corresponds to the diagonal distance between the inner axes of the universal joints of each leg. The parameter $o$ represents the offset between the two axes of the universal joint. The parameter $w$ signifies the radial distance of the outer joint axes from the central axis of symmetry. Other dependent parameters include, the angle of inclination of the diagonal link with the axis of symmetry, $\alpha = \sin^{-1}(2w/l)$, and the total vertical distance between the outer two revolute joints, $h = \sqrt{l^2 - (2w)^2} + 2o$. Further details on the kinematics of the 2DPOM mechanism are available in the works of [31, 33].

As a baseline for this study, a 2DPOM mechanism constructed with a traditional approach was used. The geometric parameters were set to be $l = 45$mm, $o = 6$mm and $w = 19$mm. This mechanism was assembled by putting together custom plastic parts and commercially available stainless steel guiding pins acting as bushings. The plastic parts were fabricated in Nylon (Polyamide 12) on a ProX SLS 6100 Selective Laser Sintering (SLS) additive manufacturing machine by 3D Systems. This "traditional" version of the mechanism was compared to its flexible counterpart, whose design is described in detail in the following sections.

Figure 2 shows the CAD renderings and the real prototypes for both the traditional and flexible mechanisms. The "traditional" design is represented on the left, while the "flexible" design on the right in both sub-figures. Corresponding parts are represented with the same colors. As can be seen, the flexure-based design is considerably simpler being made with five parts instead of eleven (connection pins excluded).

To support the reproducibility of this work the CAD models and fabrication instructions of the mechanisms are provided on a dedicated GitHub repository[1].

[1] `https://www.github.com/made-iit/flex-2dpom`

Figure 2: CAD view (top) and a photograph (bottom) comparing the two implementations of the 2DPOM mechanism considered for this work.

## 2.2 Flexure Design

The authors were interested in geometries that could be obtained via AM, and more in detail with the Fused Filament Fabrication (FFF) manufacturing process, that is also sometimes referred to as Fused Deposition Modeling (FDM).

Three flexure designs were initially considered, namely:

1. the symmetric flexure hinge (a),
2. the symmetric notch hinge (b),
3. the asymmetric notch hinge (c).

These are represented in the left column of Fig.3 which also represents their need for supports at the manufacturing stage (right column).

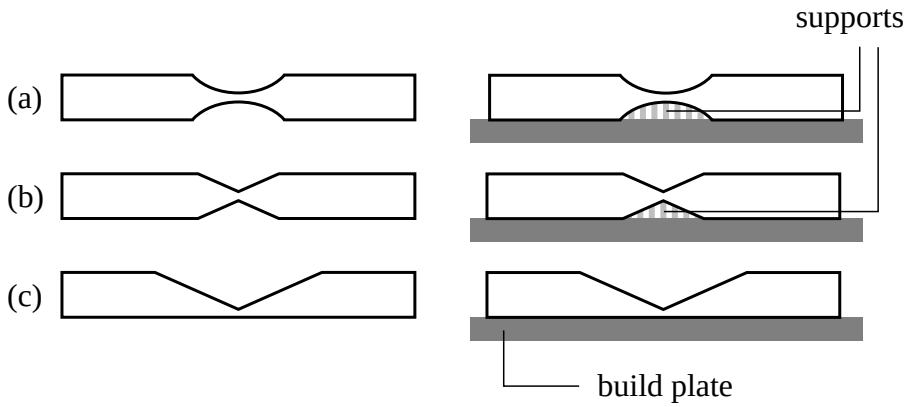


Figure 3: Flexure types.

As is known, bending flexures do not have a constant instantaneous center of rotation. However to obtain a precise positioning of the overall mechanism it was desired that the flexures approximated the rotational joints of the 2DPOM mechanism. For this reason, notch hinges were preferred for this work as most of the deformation is concentrated in the proximity of the notch.

A second aspect relates to FFF requiring the addition of supports for overhanging geometries. The addition of supports compromises the surface quality where the supports meet the part; this must be avoided in the flexure region to guarantee the highest fatigue life for the mechanism. Therefore, the asymmetric notch hinge was selected because it could be printed directly on the print bed without the need for supports. The selected flexure geometry and its main parameters being flexure width ($a$), flexure thickness ($t$) and the notch angle ($\delta$) are represented in Fig. 4.

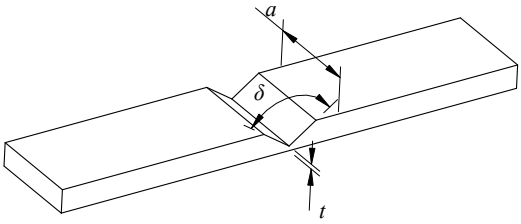


Figure 4: Flexure geometry.

It is also important to note that the notch geometry does not in practice introduce a large stress concentration as the theory of elasticity would predict. Indeed the layered slicing and manufacturing strategy of FFF, and its direction-dependent mechanical properties produce a geometry that, in the proximity of the notch, is more similar to a thin tapering beam. Fig.5 presents a conceptual representation of the layers in the proximity of the flexure notch as manufactured during the FFF process.

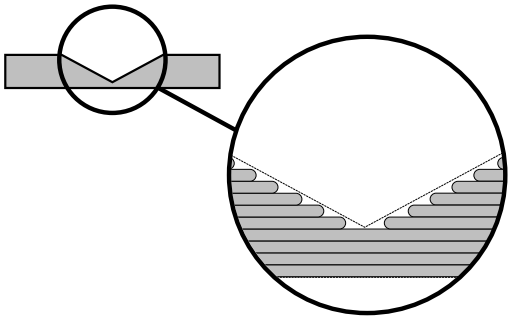

Figure 5: Notch layers manufacturing detail.

## 2.3 Manufacturing Strategy

Nylon was selected as a construction material among the available ones, because of its low Young's Modulus (hence good flexibility), and favorable resistance to stiffness ratio. Two AM systems were used for this study, the Markforged MarkTwo, and Stratasys Fortus 400mc. Flexure parts were fabricated for testing purposes with these two systems and were subjected to repeated bending. The flexures fabricated with the Stratasys Fortus 400mc failed before 10 cycles. Instead, the flexures fabricated with the Markforged MarkTwo system did not show evident signs of damage (even if inspected with magnifying equipment) even after 100 cycles of bending. These first experimentations led to conclude that the quality and durability of the

flexure depend on the minimum layer thickness that can be obtained with each printer, which is 0.1mm for the Markforged MarkTwo system, and 0.178mm for the Stratasys Fortus 400mc system. Thus, it was decided to continue with the MarkTwo system for this study.

The subsequent challenge then became the development of an appropriate flexure geometry that could be easily obtained through the manufacturing process at hand. To ensure the maximum flexure resistance all flexure axes shall be parallel to the build plane at the manufacturing stage.

The build strategy for the flexure to obtain this, is shown in Fig. 6. Figure 6(a) represents one of the three support "legs" of the mechanism on the build plane. Once each "leg" has been manufactured, it is assembled in the mechanism's neutral configuration (b). This, however, pre-strains the two inner flexures of each "leg" which are not at zero strain in the mechanism's neutral configuration.

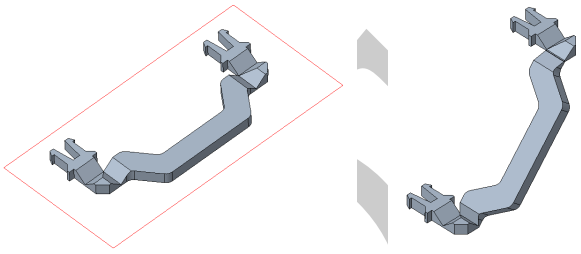

(a) (b)

Figure 6: Single "leg" manufacturing and assembly

In the region of the flexures, the slicer parameters were set such as to align the paths of the FFF extruder perpendicularly to the flexure axes thus to maximizing the flexures' resistance to bending (see Fig. 7).

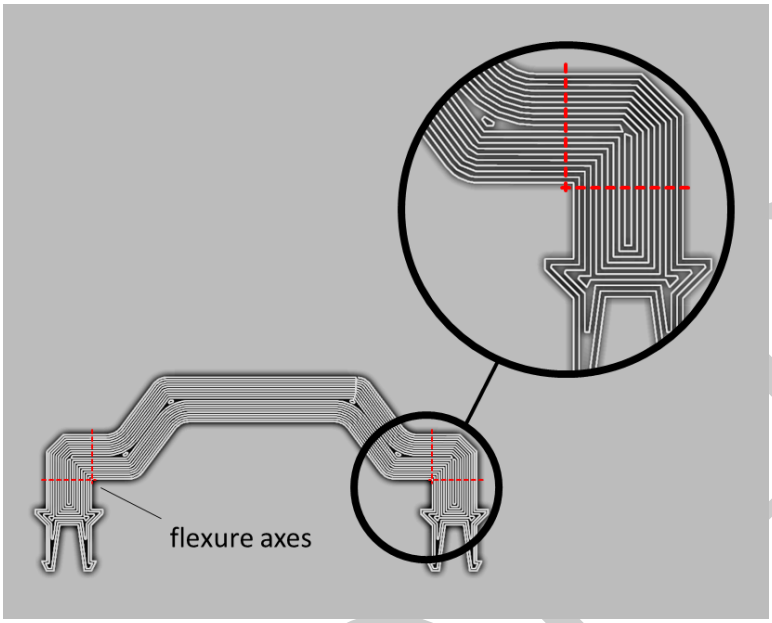


Figure 7: Extruder paths on flexure plane.

This results in a joint that is structurally rather similar to the solutions proposed in the patent by Gosselin [13], where very short and compact flexures were obtained with textiles and cables. The main difference, in this case, is that the short bending structures were fabricated with the same material as the rigid structural parts (Nylon).

An unwanted side-effect of using Nylon is that the printed part remains very flexible also during the print process, and tends to curl and detach from the printer bed, especially on large builds when the part has time to cool. To avoid this issue parts having thin sections were printed with the "brim" option activated: in this case, a series of contours are printed around the actual part to improve its adhesion to the print bed.

The initial design was subsequently optimized iteratively by building physical prototypes and subjecting them to the motions they would experience when integrated into the 2DPOM mechanism. The final design of the flexures in this study had a flexure thickness $t$ of 0.5mm, a flexure width $a$ of 4.0mm, and a notch angle $\delta$ of 100°.

## 2.4 FEM Simulations

The behavior of the notch flexure under deformation was analyzed in detail with the use of Finite Element Analyses (FEA). All analyses were conducted with the Ansys

2020 R1 software suite. The geometric model was developed within the SpaceClaim environment, whereas the FEA were conducted in the Ansys Mechanical environment. Static structural analyses under large deformations were selected for the simulations. The material Young's Modulus was set to 380MPa, and Poisson's ratio to 0.42, to simulate the physical properties of PA12. The boundary conditions are represented in Fig.8. The displacements of the left terminal face of the structure were fully constrained to zero (purple surface in Fig.8). A rotation displacement boundary condition was instead applied to the right face (yellow surface in Fig.8), while leaving the other nodal DOF free.

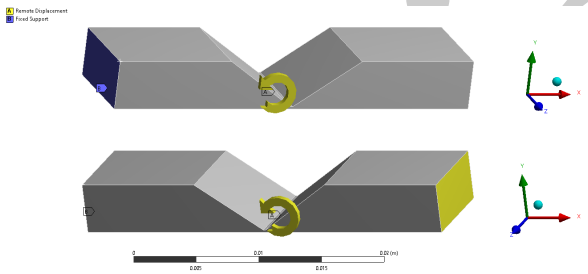

Figure 8: Boundary conditions.

The model was meshed with a mapped hex-mesh with approximately 247500 elements having a characteristic element size of $1.6e^{-4}$mm. Figure 9 represents the FEA mesh (top) and its detail at the vertex of the notch region (bottom).

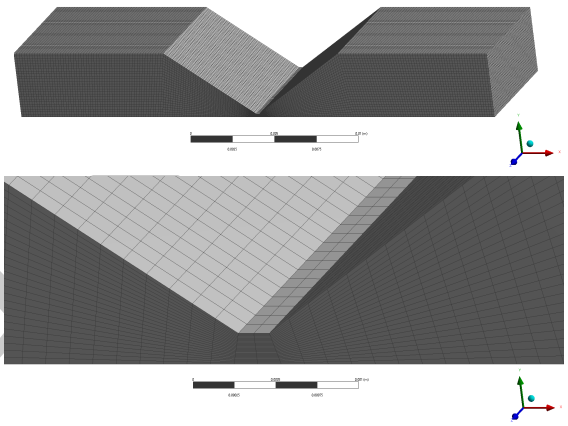

Figure 9: FEA mesh.

The applied displacement was progressively increased from 0° to 90°with 10° steps.

Figure 10 displays the result of the simulation in terms of Von Mises equivalent stress for the hinge at the 60° intermediate step.

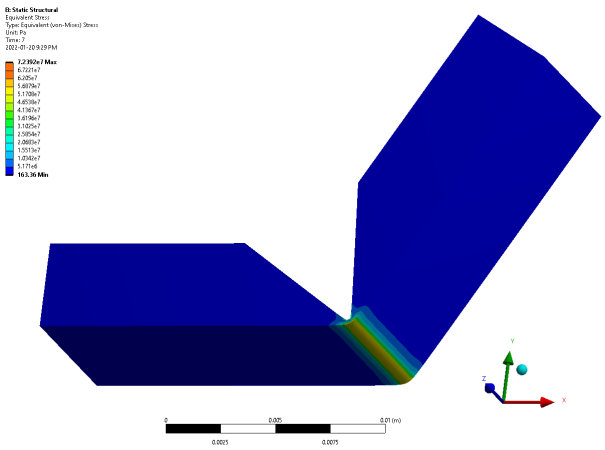


Figure 10: FEA results.

The results of the analysis were extracted and plotted in Fig.11 which represents the flexure's maximum Von Mises equivalent stress (top) and the magnitude of the displacement of the moving face from the rotation (bottom), as a function of the flexure's deflection.

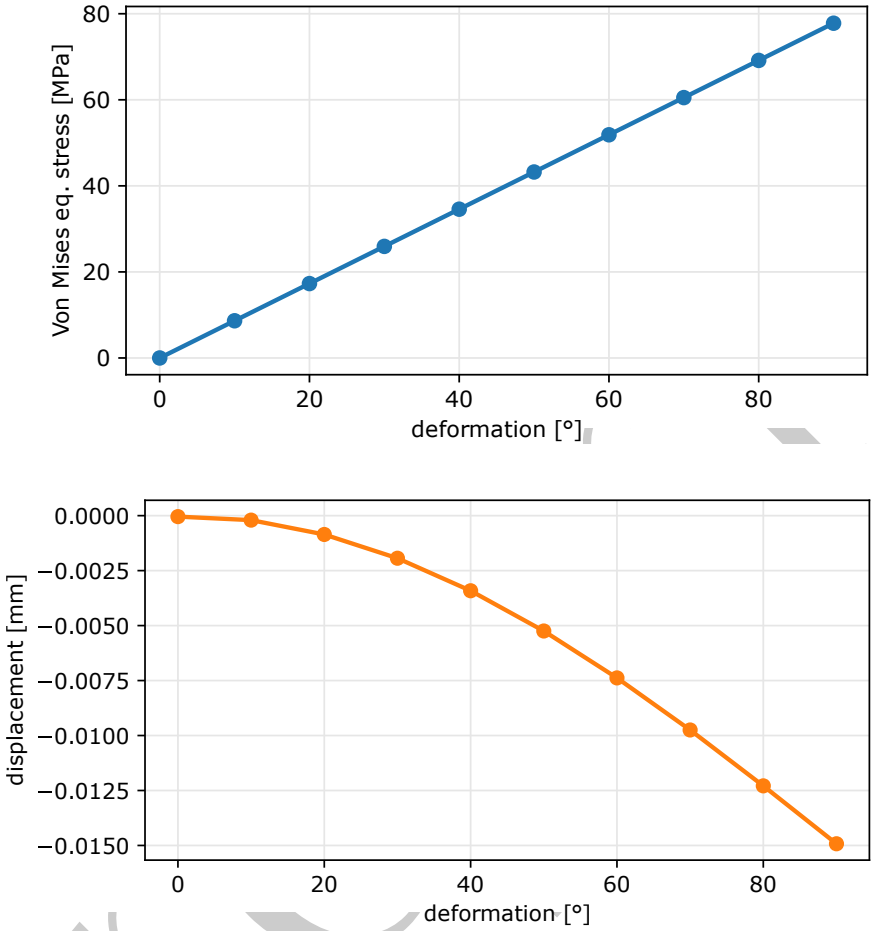


Figure 11: FEA results.

As can be seen, the radial displacement remains below $-1.5e^{-2}$mm in all angular configurations. The selected flexure geometry, therefore, nicely approximates a rotational hinge.

The maximum Von Mises stress reaches a value of 77MPa at 90° which exceeds the theoretical mechanical resistance of the material (generally 48MPa to 53MPa) of approximately 33%. This result is not in alignment with those obtained by experimentation on the physical prototype that instead resists cyclic loading at full deflection. The mismatch can possibly be explained by the orthotropic behaviour of additively manufactured materials; indeed this aspect was not modeled in detail in the current set of simulations.

## 2.5 Experimental Validation

### 2.5.1 Backlash assessment

To assess the backlash within both mechanisms, they were subjected to a particular actuator trajectory multiple times and the corresponding platform motions for each repetition were observed. One of the actuators was moved from zero configuration to maximum limit in one direction and back. This also corresponds to the platform reaching the maximum tilt and back, while keeping the azimuth constant. This motion was repeated five times.

Since this kinematic architecture lacks a fixed instantaneous centre of rotation, measuring the platform orientations directly is not straightforward. Hence, for this experiment external sensor in the form of a motion capture system was used. More in detail, a Vicon Vantage motion tracking system was employed with Vicon Nexus data capture software. It has an accuracy of 0.017mm with root mean squared error value of 0.324mm. Tracking markers were attached at specific locations on the base and the platform to track their positions for the entire motion. The platform orientations were then extracted from the motion capture data following the Tilt & Torsion paramterization [34],[32].

### 2.5.2 Loading test

Subsequently, a loading test of the two mechanisms was performed to provide a qualitative representation of their response under load. Both mechanisms were compressed, in their zero-configuration, with a Zwick-Roell ProLine Z050/TN BT1-FB050TN.D30 testing machine (see Fig. 12 which represents the "flexible" version of the mechanism prior to compression testing). The mechanisms were first compressed gradually to 30N with a cross-bar speed of 5mm/min; this test was repeated five times in each condition.

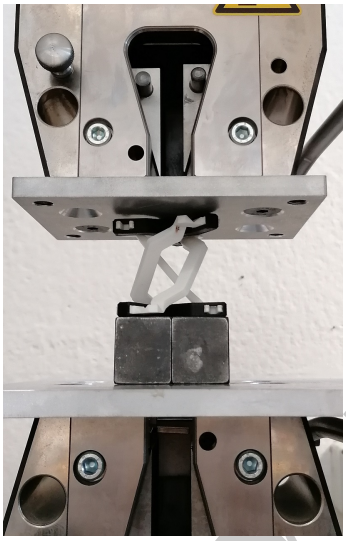

Figure 12: Load test setup.

# 3 Results and Discussion

## 3.1 Backlash assessment

Figure 13, shows the resulting platform orientations, expressed in polar coordinates $(r, \theta)$. The tilt corresponds to the radius $(r)$ of the plot where as the azimuth is the angle $(\theta)$. It can be observed that the readings for the mechanism fabricated with the traditional approach are more scattered as compared to the flexible version; this is interpreted as the flexible model having less backlash and higher precision than the traditional one. It should also be noted that the maximum tilt achieved with the flexible model is lesser as compared to the traditional model. This difference depends mainly on the different geometry of the legs, which go in self-collision earlier in one direction. This issue can, however, be mitigated by further optimizing the leg geometry.

## 3.2 Loading test

Figure 14 represents the force-displacement characteristic curves of the two versions of the mechanism. Each curve represents the average of five repetitions of the loading test. Despite its flexures, the compliant mechanism results in being stiffer, because its geometry allows constructing it with a lower $\alpha$ angle. At approximately 8.5mm of displacement, the mechanism fabricated with the traditional approach deflected until its links self-collided: further loading was deemed unnecessary. The flexure based mechanism was instead loaded until failure. The result of this test are shown in Fig.15 As can be seen, the flexible version of the mechanism can withstand

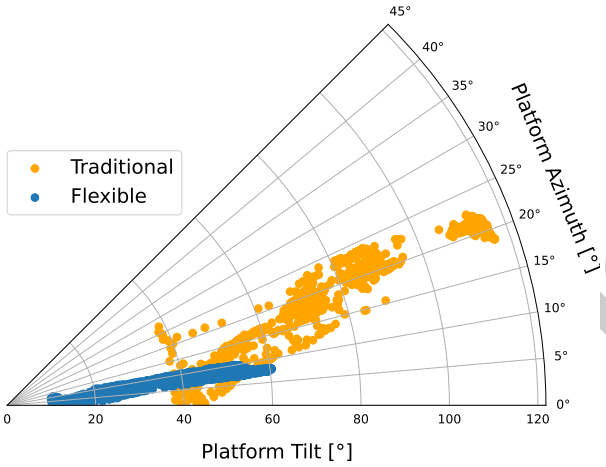


Figure 13: Results of the backlash assessment test.

up to 70N before failing. Failure occurs at the first flexure (Fig.16), that in the zero-configuration is subject to torsional loading.

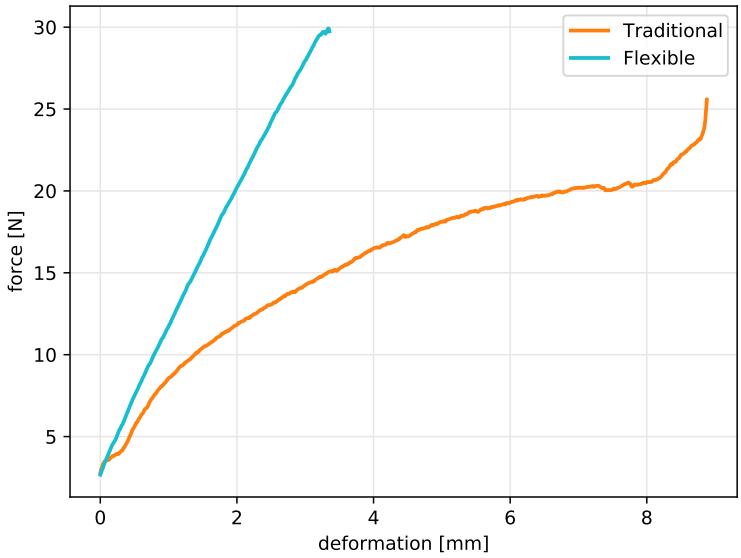


Figure 14: Comparisons of the response under load of the traditional and flexible mechanisms

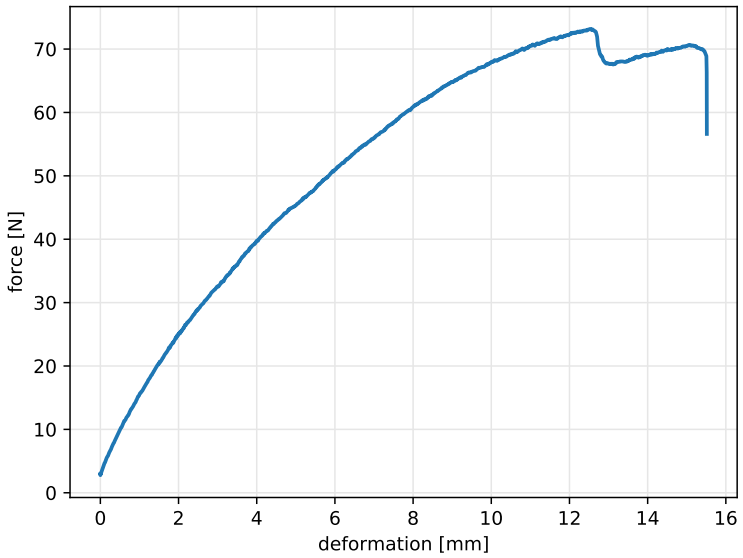


Figure 15: Force-displacement curve of the flexible mechanism when loaded until failure.

Figure 16: Failure of the flexure-based version.

# 4 Conclusions

The experiments presented in this work show how the FFF of Nylon (Polyammide12) components is a suitable approach for additively constructing flexure hinges with large displacements. Further work shall be carried out to better characterize the flexures' fatigue life as a function of the applied loads and the number of loading cycles. The adoption of AM implies manufacturing constraints on the flexure geometry; how these aspects can be dealt with at the design stage shall also be characterized more in detail. Nevertheless, the approach is promising because the mechanisms made in this way are less subject to mechanical backlash and are easier to construct and assemble being made from fewer parts. Therefore, the results presented in the current work further confirm how FFF can be considered a practical technology for fabricating small-scale parallel compliant mechanisms.

# References


[1] S. Briot and I. A. Bonev, "Are parallel robots more accurate than serial robots?" *Transactions of the Canadian Society for Mechanical Engineering*, vol. 31, no. 4, pp. 445–455, Dec 2007.

[2] L. L. Howell, *Compliant Mechanisms*. Wiley-Interscience, Aug 2001.

[3] L. L. Howell, S. P. Magleby, B. M. Olsen, and J. Wiley, *Handbook of compliant mechanisms*. Wiley Online Library, Feb 2013.

[4] N. Lobontiu, *Compliant Mechanisms: Design of Flexure Hinges*. CRC Press, Dec 2002.

[5] E. Shimada, J. Thompson, J. Yan, R. Wood, and R. Fearing, "Prototyping millirobots using dextrous microassembly and folding," *Proc. ASME IMECE/DSCD*, vol. 69, no. 2, pp. 933–940, 2000.

[6] R. J. Wood, S. Avadhanula, M. Menon, and R. S. Fearing, "Microrobotics using composite materials: The micromechanical flying insect thorax," in *IEEE Int. Conf. on Robotics and Automation (ICRA)*, vol. 2. IEEE, Sep 2003, pp. 1842–1849.

[7] A. M. Hoover and R. S. Fearing, "Fast scale prototyping for folded millirobots," in *IEEE Int. Conf. on Robotics and Automation (ICRA)*. IEEE, May 2008, pp. 886–892.

[8] A. O. Pullin, N. J. Kohut, D. Zarrouk, and R. S. Fearing, "Dynamic turning of 13 cm robot comparing tail and differential drive," in *IEEE Int. Conf. on Robotics and Automation (ICRA)*, 2012, pp. 5086–5093.

[9] D. W. Haldane, K. C. Peterson, F. L. Garcia Bermudez, and R. S. Fearing, "Animal-inspired design and aerodynamic stabilization of a hexapedal millirobot," in *IEEE Int. Conf. on Robotics and Automation (ICRA)*, 2013, pp. 3279–3286.

[10] H. McClintock, F. Z. Temel, N. Doshi, J.-s. Koh, and R. J. Wood, "The milliDelta: A high-bandwidth, high-precision, millimeter-scale delta robot," *Science Robotics*, vol. 3, no. 14, Jan 2018.

[11] M. Salerno, K. Zhang, A. Menciassi, and J. S. Dai, "A novel 4-DOF origami grasper with an SMA-actuation system for minimally invasive surgery," *IEEE Transactions on Robotics*, vol. 32, no. 3, pp. 484–498, Apr 2016.

[12] S. Mintchev, M. Salerno, A. Cherpillod, S. Scaduto, and J. Paik, "A portable three-degrees-of-freedom force feedback origami robot for human–robot interactions," *Nature Machine Intelligence*, vol. 1, no. 12, pp. 584–593, Dec 2019.

[13] F. Gosselin, "Jointed limb comprising fibres, and jointed structure and robot or haptic interface comprising such a jointed limb," U.S. patentus US20 090 260 473A1, Oct, 2009. [Online]. Available: https://patents.google.com/patent/US20090260473A1/en

[14] S. Henein, P. Spanoudakis, S. Droz, L. I. Myklebust, and E. Onillon, "Flexure pivot for aerospace mechanisms," in *10th European Space Mechanisms and Tribology Symposium*. Citeseer, 2003, pp. 285–288.

[15] M. Naves, M. Nijenhuis, W. Hakvoort, and D. Brouwer, "Flexure-based 60 degrees stroke actuator suspension for a high torque iron core motor," *Precision engineering*, vol. 63, pp. 105–114, May 2020.

[16] F. Calignano, D. Manfredi, E. P. Ambrosio, S. Biamino, M. Lombardi, E. Atzeni, A. Salmi, P. Minetola, L. Iuliano, and P. Fino, "Overview on Additive Manufacturing Technologies," *Proceedings of the IEEE*, vol. 105, no. 4, pp. 593–612, Apr 2017.

[17] R. M. Fowler, A. Maselli, P. Pluimers, S. P. Magleby, and L. L. Howell, "Flex-16: A large-displacement monolithic compliant rotational hinge," *Mechanism and Machine Theory*, vol. 82, pp. 203–217, Dec 2014.

[18] E. G. Merriam, J. E. Jones, S. P. Magleby, and L. L. Howell, "Monolithic 2 dof fully compliant space pointing mechanism," *Mechanical Sciences*, vol. 4, no. 2, pp. 381–390, 2013.

[19] L. Kiener, H. Saudan, F. Cosandier, G. Perruchoud, and P. Spanoudakis, "Innovative concept of compliant mechanisms made by additive manufacturing," *MATEC Web of Conferences*, vol. 304, p. 07002, Jan 2019.

[20] F. Parvari Rad, R. Vertechy, G. Berselli, and V. Parenti-Castelli, "Analytical compliance analysis and finite element verification of spherical flexure hinges for spatial compliant mechanisms," *Mechanism and Machine Theory*, vol. 101, pp. 168–180, jul 2016.

[21] M. Verotti, G. Berselli, L. Bruzzone, M. Baggetta, and P. Fanghella, "Design, simulation and testing of an isotropic compliant mechanism," *Precision Engineering*, vol. 72, pp. 730–737, 2021.

[22] P. Bilancia, G. Berselli, S. Magleby, and L. Howell, "On the modeling of a contact-aided cross-axis flexural pivot," *Mechanism and Machine Theory*, vol. 143, p. 103618, jan 2020.

[23] J. P. Sharkey, D. C. W. Foo, A. Kabla, J. J. Baumberg, and R. W. Bowman, "A one-piece 3D printed flexure translation stage for open-source microscopy," *Review of Scientific Instruments*, vol. 87, no. 2, p. 025104, Feb 2016.

[24] A. Almeida, G. Andrews, D. Jaiswal, and K. Hoshino, "The Actuation Mechanism of 3D Printed Flexure-Based Robotic Microtweezers," *Micromachines*, vol. 10, no. 7, p. 470, Jul 2019.

[25] M. Cutkosky and S. Kim, "Design and fabrication of multi-materials structures for bio-inspired robots," *Philosophical transactions. Series A, Mathematical, physical, and engineering sciences*, vol. 367, pp. 1799–813, Jun 2009.

[26] R. R. Ma, J. T. Belter, and A. M. Dollar, "Hybrid deposition manufacturing: design strategies for multimaterial mechanisms via three-dimensional printing and material deposition," *Journal of Mechanisms and Robotics*, vol. 7, no. 2, May 2015.

[27] S. Bailey, J. Cham, M. Cutkosky, and R. Full, "Biomimetic robotic mechanisms via shape deposition manufacturing," *Robotics Research: The Ninth International Symposium*, Jan 2000.

[28] A. M. Dollar and R. D. Howe, "A robust compliant grasper via shape deposition manufacturing," *IEEE/ASME Transactions on Mechatronics*, vol. 11, no. 2, pp. 154–161, 2006.

[29] A. Bruyas, F. Geiskopf, L. Meylheuc, and P. Renaud, "Combining multimaterial rapid prototyping and pseudo-rigid body modeling for a new compliant mechanism," in *2014 IEEE International Conference on Robotics and Automation (ICRA)*. IEEE, May 2014, pp. 3390–3396.

[30] J. A. E. Hughes, P. Maiolino, and F. Iida, "An anthropomorphic soft skeleton hand exploiting conditional models for piano playing," *Science Robotics*, vol. 3, no. 25, 2018.

[31] Y.-J. Kim, J.-I. Kim, and W. Jang, "Quaternion Joint: Dexterous 3-DOF Joint representing quaternion motion for high-speed safe interaction," in *IEEE/RSJ Int. Conf on Intelligent Robots and Systems (IROS)*. IEEE, Oct 2018, pp. 935–942.

[32] D. Shah, Y. Wu, A. Scalzo, G. Metta, and A. Parmiggiani, "A comparison of robot wrist implementations for the iCub humanoid," *Robotics*, vol. 8, no. 1, p. 11, Feb 2019.

[33] D. Shah, "Design of wrist and forearm mechanisms for enhanced humanoid dexterity," Ph.D. dissertation, University of Genoa, 2021.

[34] I. A. Bonev and J. Ryu, "Orientation workspace analysis of 6-DOF parallel manipulators," in *Proceedings of the ASME 1999 Design Engineering Technical Conferences*, vol. Volume 1: 25th Design Automation Conference. ASME, Sep 1999, pp. 281–288.